Original Research Article

Assessment of the role of translationally controlled tumor protein 1 (TPT1/TCTP) in breast cancer susceptibility and ATM signaling

Katharina Neuhäuser [a,*,1], Leonie Küper [a,b], Hans Christiansen [a], Natalia Bogdanova [a]

[a] Radiation Oncology Research Unit, Hannover Medical School, Carl-Neuberg Str. 1, 30625 Hannover, Germany
[b] Gynaecology Research Unit, Hannover Medical School, Carl-Neuberg Str. 1, 30625 Hannover, Germany

ARTICLE INFO

ABSTRACT

Background and purpose: The translationally controlled tumor protein 1 (TPT1/TCTP) has been implicated in the intracellular DNA damage response. We tested the role of TPT1 in breast cancer (BC) predisposition and re-evaluated its function in Ataxia-Telangiectasia mutated (ATM)-mediated damage recognition and DNA repair.

Material and methods: The TPT1 coding sequence was scanned for mutations in genomic DNA from 200 breast cancer patients. TPT1 was down-regulated through siRNA in breast epithelial and fibroblast cell cultures. ATM activation after irradiation (IR) was analyzed by western blotting, and γH2A.X foci were monitored by immunocytochemistry.

Results: The sequencing study identified a novel, potentially damaging missense mutation in a single patient. Silencing of TPT1 did not significantly affect ATM kinase activity and did not impair the initial formation of γH2A.X foci, while we observed a marginally significant effect on residual γH2A.X foci at 6–48 h after IR.

Conclusions: TPT1 does not harbor common mutations as BC susceptibility gene. Consistently, TPT1 protein is not required for the recognition of radiation-induced DNA damage via the ATM-dependent pathway and has only slight impact on timely repair. These results may be important when considering TPT1 as a DNA damage marker.

1. Introduction

The translationally controlled tumor protein (TPT1, also known as TCTP, fortilin, p23 or histamine releasing factor/HRF) is ubiquitously expressed in all eukaryotic cells, evolutionary highly conserved and involved in several cellular processes [1]. It is also known to play a role in the mammalian immune system and dysregulation has been implicated in a variety of cancers, also at later stages like invasion and metastasis (as reviewed in [2]). The level of TPT1 mRNA depends on cell type, developmental stage and extracellular stimuli [3]. TPT1 has been identified as an important factor in tumor reversion [4,5], is highly expressed in tumor tissues, especially of epithelial origin [1], and promotes cell migration, invasion and metastasis via induction of epithelial to mesenchymal transition [6]. The transcription of TPT1 can be positively regulated by DNA damaging agents like etoposid and cisplatin, while it is nega-

tively regulated by p53 [7]. TPT1 overexpression can lead to p53 degradation and loss of p53-mediated apoptosis [8], whereas p53 can downregulate TPT1 levels [4]. While the antagonistic effect on p53 would suggest an oncogenic function, Zhang et al. (2012) have reported that TPT1 interacts with p53 to inhibit cellular proliferation in irradiated cells [9]. Furthermore, low-dose γ irradiation enriched TPT1 in nuclei of normal human cells and its upregulation appeared dependent on ATM and the DNA-dependent protein kinase (DNA-PK). In that study, TPT1 formed a complex with ATM, phosphorylated histone H2AX (γH2A.X) and p53 binding-protein 1 (53BP1), exhibited a protective effect on irradiated cells and thus may play an important role in the maintenance of genomic integrity. However, a recent proteomics study did not identify these proteins as part of the TPT1 interactome in HeLa cells [10]. Furthermore, it has been demonstrated that the protein level of TPT1 is increased in breast cancer tissue [11], similar to what has been described for cancers of colon, liver, prostate, skin and throat [7]. While TPT1 is being considered as both marker and prognostic factor for breast cancer, its molecular impact is still incompletely understood [12]. The known interaction of TPT1 with breast cancer-associated proteins like p53 [12], the E3 ubiquitin

---

ligase HDM2 [12,13] or the FA Complementation Group A (FANCA) [14] suggests a breast cancer-related role of TPT1. We aimed to address the question whether mutations in *TPT1* were present in breast cancer patients, who have lived in areas with radiation contamination, and whether *TPT1* would classify as a breast cancer susceptibility gene, especially in the context of high radiation exposure due to its cytoprotective function [9]. Furthermore, we sought to investigate whether the proposed role of TPT1 in DNA double strand break repair could be employed in its use as a DNA damage marker after ionizing radiation.

2. Materials and Methods

2.1. Patients

The patient cohort consisted of 200 female patients with BC who lived in Belarusian regions contaminated due to the Chernobyl incident in 1986. They were selected from a larger group of 1759 BC patients of the Hannover-Minsk Breast Cancer Study (HMBCS) by choosing women from regions with increased ground contamination [15]. The cumulative total effective whole-body radiation dose for every selected patient was estimated between 10 and 45 mSv. For direct genotyping of one newly detected variant, another group of 500 BC patients from Belarus was randomly selected from the same series.

2.2. TPT1 sequencing

Genomic DNA was extracted from peripheral blood leukocytes of patients using proteinase K digestion and phenol–chloroform extraction. To analyze the cohort (n = 200) for *TPT1* gene variants, primer pairs were designed to specifically flank all six coding exons of the gene (Supplementary Table S1). PCR was used to amplify the genomic DNA fragments and, after purification of the products, direct sequencing using BigDye v1.1 terminator chemistry and a 3100 Avant capillary sequencer (Life Technologies) was performed. Sequencing data were analyzed with the Sequencing Analysis 5.1.1 software.

2.3. High resolution melting (HRM)

Identified *TPT1* variants in 200 selected breast cancer patients were tested for their frequencies in a larger series (n = 500) of HMBCS. New primers were designed to specifically scan the variant-containing amplicons in all randomly selected 500 samples (Supplementary Table S1). Labelling of DNA was performed by Eva-Green qPCR MasterMix (Biotrend, Exton, USA) and melting profiles were analyzed with the Rotor-Gene 6000 HRM 2-Plex Software (Qiagen, Venlo, Netherlands).

2.4. Bioinformatics

Identified variants were matched with database information in the NCBI SNP database (www.ncbi.nlm.nih.gov/SNP), the 1000 Genomes Browser (browser.1000genomes.org), the ExAC Browser (http://exac.broadinstitute.org/), the Tumorportal (www.tumor-portal.org), the cBio Portal for Cancer Genomics (http://www.cbio-portal.org/) and the Catalogue of Somatic Mutations in Cancer (COSMIC v71, www.cancer.sanger.ac.uk). The programs SIFT (sift.jcvi.org/), PROVEAN (provean.jcvi.org/), MutationTaster (www.mu-tationtaster.org) and PolyPhen-2 (http://genetics.bwh.harvard.edu/pph2/) were used to predict the pathogenicity of the variant. MaxEntScan (http://genes.mit.edu/burgelab/maxent/Xmax-entscanscoreseq.html) and ESEfinder 3.0 (rulai.cshl.edu/tools/ESE/) were used to identify potential alternative splice sites.

2.5. Cell culture

Cell lines were obtained from the American Type Culture Collection (ATCC) or established from patient material. Human breast epithelial MCF10A cells (CRL-10317[TM]) were cultured in MEBM supplemented with MEGM Single Quots according to the manufacturer's instructions (Lonza/Clonetics). Human triple negative BC cell lines HCC1395 and HCC1937 (CRL-2336[TM] and CRL-2324[TM], respectively) were cultured in RPMI 1640 with 10% fetal calf serum (FCS), 500 U/ml penicillin, 0.5 mg/ml streptomycin and 2 mM L-glutamine. Wild-type TERT-immortalized human skin fibroblasts BJ5TA (ATCC, CRL-4001) were cultured in DMEM (Sigma) with 10% fetal calf serum (FCS), 500 U/ml penicillin, 0.5 mg/ml streptomycin, 2 mM L-glutamine and 10 µg/ml hygromycin B. Normal human fibroblasts from a healthy individual, ADP, were kindly provided by Professor Detlev Schindler (University of Würzburg) after immortalisation with SV40 large T, and were cultured in DMEM (Sigma) with 10% FCS, 500 U/ml penicillin, 0.5 mg/ml streptomycin and 2 mM L-glutamine. All cells were grown at 37 °C in a humidified atmosphere supplemented with 5 %CO$_2$. Independent experiments for biological replicates were performed at least twice.

2.6. siRNA silencing

siRNAs capable of targeting *TPT1* were obtained from Ambion (AM16708A #284697, #13153, #289422) and were used as steady mixture [9]. Scrambled (Scr) siRNA Duplex (Ambion) was included as control, and reverse transfection with Lipofectamine[TM] RNAi-MAX (Invitrogen, #13778) was used to apply siRNAs to subconfluent cells 48 h prior to irradiation (IR).

2.7. ATM-Inhibition

One hour before IR the cells were treated with the ATM inhibitor Ku55933 (KuDos Pharmaceuticals, Cambridge, UK) at 2 µM or 10 µM, respectively, in DMSO. Control cells were treated with DMSO only.

2.8. Irradiation

Ionizing radiation with doses between 60 mGy and 6 Gy was applied to the cells at room temperature using an Elekta Synergy accelerator (Siemens, Munich, Germany). The energy of the X-radiation was 6MVX and a dose-rate of 400 MU/min was applied to the cells.

2.9. Lysate preparation and immunoblotting

For preparation of protein extracts, cells were lysed in cell extraction buffer (50 mM Tris-HCl pH 7.4, 150 mM NaCl, 2 mM EGTA, 2 mM EDTA, 25 mM NaF, 25 mN beta-glycerophosphate, 0.1 mM Na$_3$VO$_4$, 0.1 mM PMSF, 5 µg/ml leupeptin, 1 µg/ml aprotinin), 0.2% Triton X-100, 0.3% NonidetP-40 for 45 min on ice. Protein extracts were cleared through centrifugation at 19500xg (13200 rpm) for 15 min, and supernatants were separated through SDS-PAGE and transferred to nitrocellulose membranes by wet blot technique. Antibodies to TPT1 (Abcam, #ab133568, 1:50000), p-KAP1 S824 (Bethyl, #A300-767A-1, 1:2000–1:5000), p-CHEK2 S19 (Cell Signalling, #2666, 1:500–1:1000), p21 (Cell Signalling, #2846, 1:1000), ATM (Epitomics, #1549–1, 1:1000), DNA-PK (Calbiochem, #NA57T, 1:600) and β-actin (Sigma, #A5441, 1:3000) were applied over night at 4 °C after blocking with 5% skim milk in PBST for 1 h. Anti-mouse and anti-rabbit horseradish peroxidase-labelled secondary antibodies were purchased from GE Healthcare. Visualization of immunoreactive bands was performed with ECL and X-ray films.

2.10. Subcellular fractionation

For cytoplasmic, nuclear and chromatin-bound protein isolation, cells were lysed in buffer A [50 mM Hepes (pH 7.4), 10 mM KCl, 1 mM EDTA, 1 mM EGTA, 1 mM DTT, 0.5% NonidetP-40, 0.1 mM PMSF, 5 μg/ml leupeptin, 1 μg/ml aprotinin] for 10 min on ice by frequent vortexing intervals. Cytoplasmic fractions were harvested by centrifugation at 4000xg for 4 min on ice. Pellets with nuclei were washed once with buffer B [1.7 M sucrose, 50 mM Hepes (pH 7.4), 10 mM KCl, 1 mM EDTA, 1 mM EGTA, 1 mM DTT, 0.1 mM PMSF, 5 μg/ml leupeptin, 1 μg/ml aprotinin] and centrifuged for 30 min at 16000xg. To harvest nuclei, pellets were resuspended in buffer C [10% glycerol, 50 mM Hepes (pH 7.4), 400 mM KCl, 1 mM EDTA, 1 mM EGTA, 1 mM DTT, 0.1 mM PMSF, 5 μg/ml leupeptin, 1 μg/ml aprotinin] and incubated 30 min on ice with frequent vortexing. Soluble nuclear proteins were separated from insoluble chromatin by centrifugation at 16000xg for 5 min at 4 °C. The final chromatin pellet was resuspended in 1 U/μl DNase I (Roche, #92161121) in buffer C and incubated for 30 min at 37 °C to release chromatin-bound proteins. Subsequent centrifugation at 1300xg for 15 min at 4 °C was applied to harvest chromatin-bound proteins in the supernatant.

2.11. Immunocytochemistry

Cells grown on cover slips in six-well plates were fixed with 3% (w/v) PFA, 2% (w/v) sucrose in PBS for 10 min. Permeabilization was performed with 0.2% (v/v) triton X-100 in PBS. Antibodies against TPT1 (Abcam, #ab133568, 1:200–1:250 or Abcam, #ab37506, 1:200–1:250, respectively), Histone H2A.x Phospho (S139) (γH2A.X) (Millipore, #05-636, 1:200), 53BP1 (Bethyl Laboratories, A300-272A, 1:200) and RAD51 (Genetex, GTX70230, 1:200) were incubated in 2% (w/v) normal goat serum (Dianova) for 2 h. After PBS washing, cells were incubated with Alexa Fluor Anti-mouse IgG 488 (Invitrogen, #A11018) and Alexa Fluor Anti-rabbit IgG 546 (Invitrogen, #A11071) or FITC-conjugated Anti-mouse IgG antibody (Zymed, #62–6511) and Alexa Fluor Anti-rabbit IgG 488 (Invitrogen, #A11070) for 2 h. DNA was counterstained with DAPI (Invitrogen) and cells were mounted with ProLong® Gold (Invitrogen). Images were taken with a Leica DMI6000B microscope (40x–63x magnification) or, for a more detailed inspection, using an Olympus confocal microscope FV 1000 (60x magnification). γH2A.X and 53BP1 foci were counted manually with Image J software in an average of 100 cells after siRNA treatment and IR for each of two independent experiments (γH2A.X), independent from the cell-cycle phase. Cells with apoptotic morphology or cells with intensely and completely stained nucleus were excluded from the counting process. For pre-extraction, cells were subjected to detergent extraction with a buffer containing 10 mM Hepes (pH 6.8), 100 mM NaCl, 300 mM sucrose, 3 mM MgCl₂, 1 mM EGTA and 0.5% triton X-100 in PBS for 5–10 min to remove the majority of non–chromatin-bound proteins before fixation and immunostaining [9]. Colocalization was defined as yellow stained dots in overlay pictures generated with confocal microscopy. In general, the "colocalization rate" was very low, but at least 10 "colocalization-positive" cells were examined and counted manually in control cells and at least 15 cells in irradiated samples, respectively.

2.12. Statistics

All experiments were performed at least two times and comparisons between treatment groups and respective controls were conducted using unpaired two-tailed t-test by GraphPad Prism version 5.00 for Windows, GraphPad Software, San Diego California, USA. Regression analyses and three-way ANOVA were performed using STATA12. P values < 0.05 in the pairwise comparison of groups or in interaction analyses were considered significant.

3. Results

### 3.1. Evaluation of TPT1 as a candidate breast cancer susceptibility gene

Given increased TPT1 levels in BC cells or BC tissues [11,16,17] and its possible role in DNA repair, we sought to investigate whether mutations in TPT1 were enriched in breast cancer patients. The six coding exons of TPT1 were amplified from an exploratory series of 200 genomic DNA samples of breast cancer patients from the HMBCS [18] and were subjected to mutation identification through Sanger sequencing. We identified a novel missense substitution, c.452A > G resulting in a Tyr to Cys substitution p.Y151C (Fig. 1A) in one patient and a previously recorded synonymous variant, c.492G > A, in another patient. Both mutational changes were not detected in additional 500 breast cancer cases scanned via HRM analysis of the respective exons (Fig. 1B), indicating that germline mutations in TPT1 were rare events in breast cancer patients from our series. The c.452A > G variant affects a beta sheet structure close to the binding domain of TPT1 protein [13] (Fig. 1C), and was predicted to be pathogenic by SIFT, PROVEAN and MutationTaster (Fig. 1D-E and Supplementary Fig. S1). SIFT predicted a pathogenic impact of p.151Y > C with a "Median Information Content" of 2.78 and a score of 0.01 [19]. Analysis with PROVEAN confirmed this result and also predicted pathogenity with a score of −6.301, which is below the threshold of ≤−2.5 [20] (Fig. 1D–E). We could furthermore confirm this result with the software MutationTaster, which classified this mutation to be "disease causing" as protein structures might be affected because the exchanged amino acids differ highly (score = 194 of maximum 215), see Supplementary Fig. S1. Furthermore, a high conservation of this area was predicted by the tools PhyloP (score = 1.01) and PhastCons (maximum score of 1), however no impact on splice sites was found. A score of 0.9999 demonstrated a high accury of this method (range 0–1) [21]. Analysis by Polyphen-2 predicted no pathogeneity for this mutation with a sensitivity of 0.93, a specificity of 0.85 and a score of 0.083 [22]. A comparison of sensitivity, specifity and accuracy of the applied software tools is given in Fig. 1F [23].

3.2. Role of TPT1 for ATM signaling in human skin fibroblasts and breast epithelial cells

Previous data on human primary cells strongly supported a role of TPT1 in DNA damage sensing and repair processes [9]. To investigate whether TPT1 is required for ATM signaling, we silenced TPT1 by siRNA in large T immortalized human skin fibroblasts (ADP) and in spontaneously immortalized human breast epithelial cells (MCF10A) [24], and investigated the phosphorylation of ATM target proteins KAP1 (at Ser824) [25–28] and CHEK2 (at Ser19) [29] in response to low (60 mGy) or high (6 Gy) dose irradiation. Furthermore, as Zhang et al. reported a defect in p21 activation following TPT1 knockdown [9], analyses of the p21 level after TPT1 depletion were performed (Supplementary Fig. S2A), and only revealed a visible increase of p21 levels in ADP cells 30 min after 6 Gy IR, while p21 levels in MCF10A remained largely unchanged. At 30 min post-irradiation, KAP1 pS824 (Fig. 2) and CHEK2 pS19 (Supplementary Fig. S2B) were easily detected in both cell lines but neither line showed differences in phosphorylation levels of both ATM targets after TPT1 knockdown compared to scrambled controls. These experiments indicated that TPT1 levels exert no gross influence on ATM kinase activity towards these substrates. Furthermore, TPT1 knockdown did not influence ATM levels (Sup-
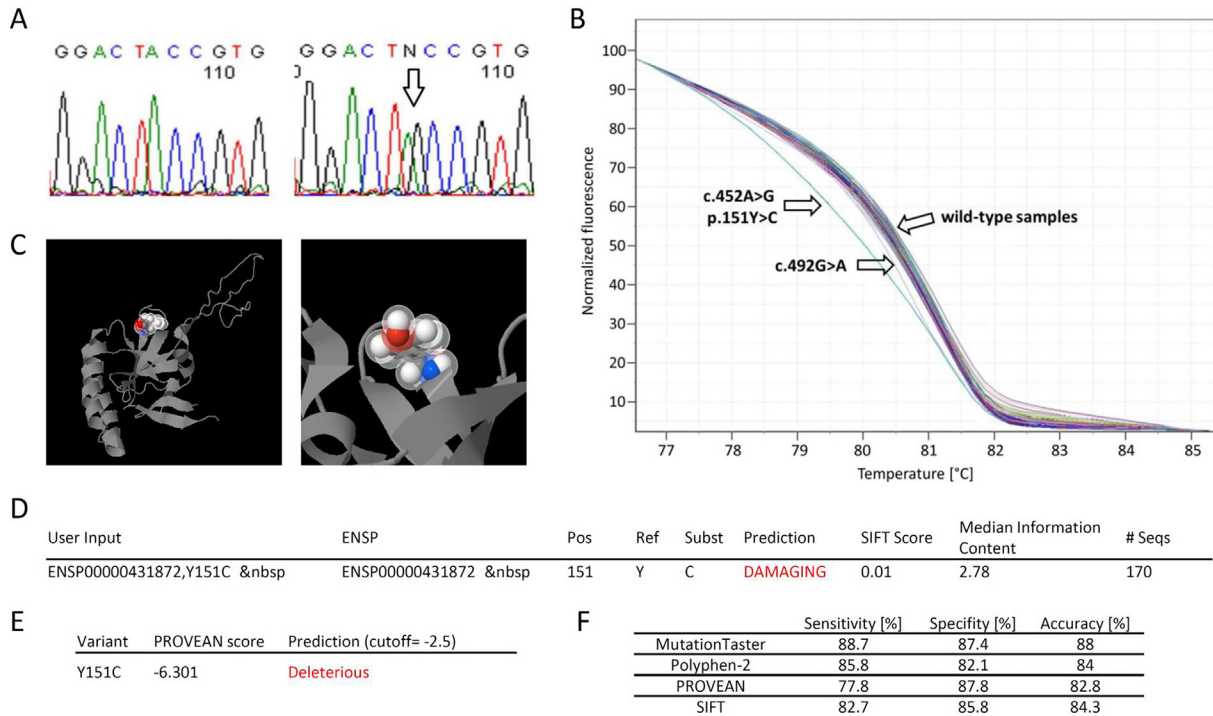
Fig. 1. Identification, screening and prediction of functional impact of c.452A > G (p.Y151C). A: Identification of mutation c.452A > G (p.Y151C) by Sanger sequencing in a heterozygous breast cancer patient (right, arrow) compared with the wild-type sequence (left). B: High Resolution Melting analysis showing melting curves of the two variants c.452A > G (p.Y151C), c.492G > A, and wild-type samples. C: 3D-model of TPT1 by Polyphen-2 showing altered amino acid as part of a beta sheet structure. D,E: Prediction results by SIFT-analysis (D) and PROVEAN-analysis (E) showing damaging impact of c.452A > G (p.Y151C) F: comparison of prediction tool performance.
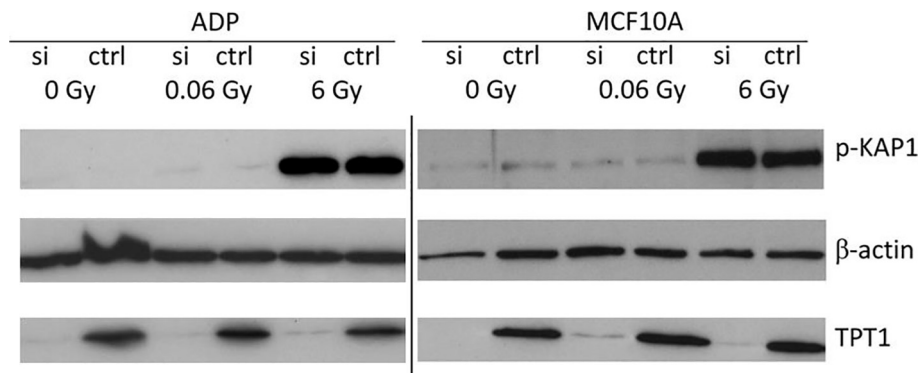

Fig. 2. Knockdown of TPT1 does not influence ATM signaling by means of KAP1 (S824) phosphorylation. Western blots of ADP and MCF10A cells treated with *TPT1* siRNA (si) or scrambled control (ctrl) 48 h prior to IR and lysed 30 min after no (0 Gy), low dose (0.06 Gy) or high dose (6 Gy) IR. The immunoreactivies of KAP1 pS824, TPT1 and β-actin as loading control are shown.

plementary Fig. S2C) and *vice versa*, ATM kinase inhibition with the specific inhibitor Ku55933 did not affect TPT1 levels, while there was strong reduction in phosphorylation of the ATM target KAP1 (Supplementary Fig. S2D). Levels of TPT1 also did not change at 30 min after low or high dose IR in whole cell extracts from ADP, MCF10A and the triple negative BC cell lines HCC1395 and HCC1937 (Supplementary Fig. S3A-B).

3.3. Intracellular distribution of TPT1 after irradiation in human skin fibroblasts and breast epithelial cells

As TPT1 is both a cytosolic and a nuclear protein, we next examined whether the intracellular localization pattern of TPT1 after IR may change according to a functional recruitment of TPT1 in DNA damage sensing and repair processes. We analyzed the intracellular distribution of the protein by cellular fractionation (Supple-

mentary Fig. S3C) as well as by immunofluorescence (Fig. 3; Supplementary Figs. S4–S8). The specificity of the immunofluorescence staining was validated with two different TPT1 antibodies (Fig. 3A and B; Supplementary Figs. S4–S7) at 1 h after IR. We could not detect gross changes in TPT1 localization at 1 h after low (0.06 and 0.25 Gy), intermediate (1 Gy) or high doses (6 Gy) of IR, respectively, when assessed in asynchronous subconfluent cells. Foci-like structures of TPT1 were visible by confocal analyses, which appeared in both cytoplasm and nucleus in irradiated and control cells (see also Supplementary Fig. S8C for ADP cells). Immunostainings in triple negative BC cell lines (Supplementary Fig. S8A-B, and data not shown) also provided no evidence for nuclear translocation of TPT1 at 1 h after IR with 0.25 Gy and 1 Gy (Supplementary Fig. S8A-B) or 0.06 Gy and 6 Gy (data not shown), respectively. Consistent with this data, we did not find robust evidence for chromatin binding of TPT1 in ADP or MCF10A cells prior or 30 min after
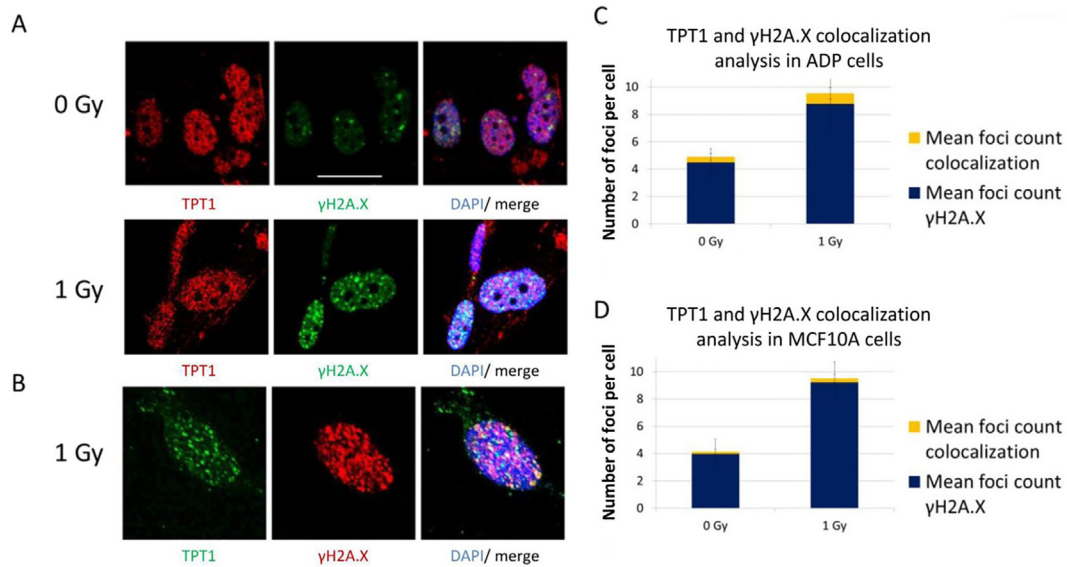
Fig. 3. No evidence for colocalization of TPT1 and γH2A.X in ADP and MCF10A cells. Asynchronous, subconfluent cells were pre-extracted with Triton X-100 (9) and fixed 1 h after IR. Panel A shows immunofluorescence stainings for TPT1 (red) (ab37506) and γH2A.X (green) in ADP cells and areas of colocalization are visible in yellow in the overlay picture. Scale bar = 25 µm. For comparison, TPT1 staining in ADP cells was performed with a second antibody (ab133568) visualized in green which is shown in panel B after 1 Gy IR. γH2A.X foci and areas of colocalization were counted manually and shown as means with standard deviations for ADP in panel C and MCF10A cells in panel D.

IR with 60 mGy or 6 Gy (Supplementary Fig. S3C and data not shown). KAP1 was phosphorylated and present in cytosolic, nuclear and chromatin-bound fractions as expected. In contrast, TPT1 was only present in cytosolic and nuclear fractions and not chromatin-bound, independent of treatment, and its localization did not detectably change after IR. These findings supported our immunofluorescence data for ADP and MCF10A (Fig. 3; Supplementary Figs. S4–S7, S8C), HCC1937 (Supplementary Fig. S8A-B), as well as HCC1395 and HCC38 (data not shown).

3.4. Limited colocalization of TPT1 with γH2A.X and RAD51 foci in different cells of human origin

Given the lack of evidence for an involvement of TPT1 in ATM signaling and its uniform intracellular distribution after IR, we analyzed whether the nuclear fraction of TPT1 shows colocalization with γH2A.X repair foci after IR. In order to reduce cytoplasmic background staining, cells were subjected to a preextraction procedure with Triton X-100 prior to fixation [9]. Cells were analyzed at 1 h after 1 Gy IR, with stainings for TPT1 and γH2A.X also being performed in TPT1 knockdown cells and non-preextracted cells (Supplementary Figs. S4-S7) as well as in irradiated triple negative BC cell lines (see Supplementary Fig. S8A-B for HCC1937, data for HCC 1395 and HCC38 not shown). In order to validate the staining, two different TPT1 antibodies were used, one of which has already been published in this context [9]. Although both antibodies showed a spotty pattern of TPT1 in the cytoplasm as well as in the nucleus, a colocalization of TPT1 and γH2A.X was poorly detectable in either cell type under any condition. Knockdown of TPT1 in ADP and MCF10A cells was confirmed by confocal immunofluorescence analyses, in agreement with the western blot results shown in Fig. 2 (Supplementary Figs. S4 and S5). Very few areas of colocalization were detected according to the overlay of TPT1 and γH2A.X staining and were counted in accordance with γH2A.X foci. The proportion of colocalized foci is displayed as means with standard deviations in Fig. 3C for ADP and Fig. 3D for MCF10A cells and was below 10% in ADP and below 5% in MCF10A cells. Furthermore, as recent findings in human cervical cancer HeLa cells support an interaction of TPT1 with RAD51 [30], colocal-

ization of TPT1 with RAD51 foci after IR was investigated in wild-type TERT-immortalized BJ5TA cells (Supplementary Fig. S8D). In line with our results in skin epithelial, breast epithelial as well as breast cancer cell lines, we neither detected nuclear translocation nor foci formation of TPT1 after IR and no clear colocalization of TPT1 with RAD51 foci.

3.5. Knockdown of TPT1 does not impair formation of γH2A.X foci after irradiation

We next investigated the role of TPT1 in the context of γH2A.X foci formation and disassembly including early and later time points after IR. *TPT1* was silenced by siRNA in ADP and MCF10A cells and γH2A.X foci (Fig. 4) and 53BP1 foci (Supplementary Fig. S9) were counted by using immunofluorescence analysis. Regression analysis revealed a strong correlation between γH2A.X foci and 53BP1 foci in both cell lines, irrespective of *TPT1* silencing (total r^2 = 0.972, Supplementary Fig. S10). We did not observe any significant changes in γH2A.X foci numbers and 53BP1 foci numbers in *TPT1* silenced cells compared to scrambled controls in any of the cell lines at all time points. Three-way ANOVA analyses disclosed a borderline significant effect of *TPT1* silencing on γH2A.X foci ($p = 0.04$), though not on 53BP1 foci (Supplementary Table S2). These analyses were in line with the observation that *TPT1* knockdown did not significantly affect the γH2A.X and 53BP1 formation in MCF10A breast epithelial cells at any time-point (Fig. 4, Supplementary Fig. S9), while in *TPT1* silenced ADP fibroblasts, a borderline significant effect of siRNA-treatment on γH2A.X foci formation, especially at 24 h after IR, could not be finally excluded (Supplementary Tables S2 and S3). We did not observe significant changes in 53BP1 foci formation in both cell lines at all time points (Supplementary Fig. S9). A linear prediction model including both cell lines revealed marginally significant contrasts between time points in terms of treatment (Supplementary Fig. S11 and Supplementary Table S3). The data suggested subtle differences in DNA damage resolution processes after IR, though not in the early foci formation at 1 h after IR, which is partially consistent with published observations [9].
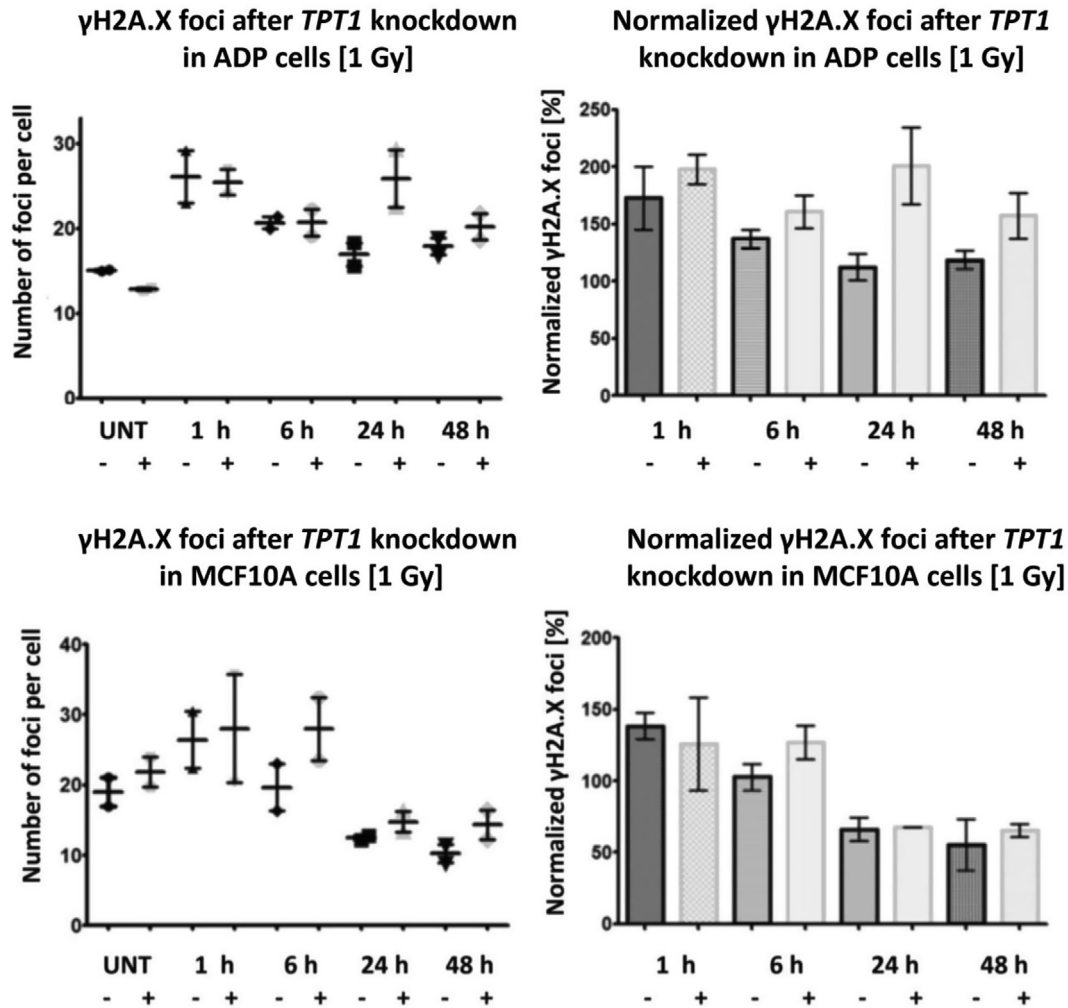
Fig. 4. γH2A.X foci numbers in TPT1 knockdown cells after irradiation. Asynchronous, subconfluent ADP and MCF10A cells were treated with siRNA against TPT1 (+, light grey columns) or scrambled controls (-, dark grey columns) 48 h before IR with 1 Gy. Cells were fixed on glass slides at 1 h, 6 h, 24 h or 48 h after IR and stained for TPT1, γH2A.X and DAPI. γH2A.X foci were counted manually in an average of 100 cells on each slide and cells with a minimum of 3 foci were considered foci-positive and subjected to counting. Foci numbers were normalized to unirradiated controls (UNT) [%] (right-hand side) and means with standard deviations from two independent experiments are shown. Original data are shown in scatter plots on the left-hand side.

4. Discussion

TPT1 has been described as biomarker for BC [31] and correlation of expression with clinical parameters of aggressive disease is high in several cancers including breast and ovarian cancer [7,12,32]. Furthermore, a positive correlation of *TPT1* overexpression with tumor size, clinical stage, lymph node metastasis and histological grade of BC is known [11]. It was therefore tempting to investigate whether *TPT1* variants also play a role in genetic breast cancer predisposition. In order to analyze whether selected BC patients, who lived for long in radiation contaminated regions, might have acquired their cancers due to mutations in the *TPT1* gene, we screened for genetic variations of *TPT1* in 200 patients from contaminated areas in Belarus. Although two mutations in *TPT1* could be detected, one of which was proposed to be pathogenic, both changes were not found in additional 500 breast cancer cases. The potentially damaging p.Y171C substitution also has not been described by the Exome Aggregation Consortium (http://exac.broadinstitute.org/gene/ENSG00000133112, accessed on December 18, 2018) and may thus represent a private mutation. We used four software tools to predict the pathogeneity of this substitution and – with the exception of Polyphen-2, all tools predicted damaging outcome. Closer investigations of the 3D structure of TPT1 have

shown that the exchanged amino acid lies within a beta sheet structure with unknown function, however, close to the binding domain of the protein, where binding to tubulin, calcium, mouse double minute 2 homolog (MDM2), the Na, K-ATPase and p53 occurs [7,13,33]. Impairment of the binding capacity of TPT1 to tubulin could disturb the cell cycle, while loss of the calcium-binding capacity of TPT1 could diminish the compensation capacity of cellular stress and favour apoptosis, which could also be enhanced through binding defects with MDM2 and p53. Furthermore, a diminished binding capacity to the Na, K-ATPase could result in reduction of cellular proliferation, however, further experiments need to clarify a possible impact of the close proximity of p.151Y > C to the binding domain of TPT1. Epidemiological aspects should be considered for both mutation carriers (p.151Y > C as well as c.492G > A), as both patients lived in areas with a cumulative total effective whole-body radiation dose of 30 mSv. The p.151Y > C carrier was diagnosed with estrogen-receptor negative infiltrating lobular carcinoma, staging code T1N0M0, at the age of 33. First, as well as second grade relatives of this patient also suffered from breast cancer, however, none of the four founder-mutations in the susceptibility genes *BRCA1* and *BCRA2* (*BRCA1**5382insC, *BRCA1**4153delA, *BRCA1**C61G or *BRCA2**6174-delT) were detected. The carrier of c.492G > A, however, was diag-

nosed with estrogen-receptor positive adenocarcinoma of grade G1 (T2N1M0) at the age of 52 with no known family history of cancer and also no mutations in BRCA1 or BCRA2. The rarity of germline TPT1 mutations in our breast cancer patients is consistent with the rarity of somatic TPT1 mutations in breast carcinomas. Only two mutations, a start codon mutation and a p.R107T substitution, have been hitherto detected in over 3000 invasive breast carcinomas (www.cbioportal.org, accessed on April 5, 2017). As mentioned above, the high TPT1 activity in some cancer types, which contributes to oncogenesis, can result from a mutation in TP53 [12]. Given the fact that the c.452A > G carrier has lived in areas with high radiation contamination, it is possible that an impairment in TPT1 function has contributed to accumulation of radiation damage and promotion of the disease. Furthermore, the functional impact of TPT1 in the DNA damage response, particularly in the context of ATM signaling, was investigated in this study. Ionizing radiation induces DNA double strand breaks that are signaled via ATM kinase which is activated rapidly after IR [34]. In its activated form, ATM can phosphorylate many downstream targets, for example KAP1, CHEK2, or the histone H2AX leading to γH2A.X [35] which then serves as a platform to recruit additional proteins working in the DNA damage response. Subsequent recruitment of further DNA repair or damage-signaling factors to the break is mediated by chromatin modification and/or direct interactions of these factors with γH2A.X [35]. The role of TPT1 in this context is presently not well understood, although TPT1 has been shown to exhibit a broad spectrum of cellular functions including apoptosis, cell survival and DNA damage sensing and repair, also in the low-dose IR context [9,36,37]. Specifically, it has been reported that TPT1 directly regulates ATM activity in Drosophila melanogaster cells [38], that IR increases TPT1 levels in nuclei of human AG1522 cells in an ATM-dependent manner, and that TPT1 colocalizes to radiation-induced foci to actively participate in DNA repair [9]. These features of TPT1 could make this protein an attractive biomarker for radiation exposure and a possible target for radiosensitisation. In our study, we did not find effects of TPT1 on ATM function at any radiation dose by assessing KAP1-phoshorylation on Ser824 in MCF10A and ADP cells, although this phosphorylation site is a main target of ATM [25–28]. We similarly observed no alterations in phospho-CHEK2 levels after TPT1 depletion. As inhibition of cell cycle progression is an important step towards repairing damaged DNA, we have analyzed whether TPT1 knockdown might influence the cell's ability to signal arrest via induction of p21. In the course of the DNA damage response, p21 is known to be activated in an ATM-p53-dependent manner, and is dependent on ATM for induction of G2 arrest [39–41], however, it can also be regulated by a p53-independent mechanism [42] (and reviewed by [43]). In both cell lines, we have detected an increase in p21 immunoreactivity after irradiation as expected, however, no influence of siRNA treatment, which underlines our hypothesis that TPT1 is not implicated in the ATM-coupled DNA damage response in our cellular systems, since protein levels of ATM were not influenced by TPT1 knockdown without and after 6 Gy IR. Although direct interactions between ATM and TPT1 have been found in cell cultures and Drosophila in vivo models after IR [9,38], a recent study in HeLa cells did not reveal ATM, 53BP1 or γH2A.X as interaction partners of TPT1 [10]. Reportedly, ATM depletion decreased TPT1 foci formation although it still translocated to the nucleus [38]. However, we found no changes of TPT1 levels in whole cell extracts after ATM inhibition and IR in both cell lines tested. The observed fraction of nuclear TPT1 was not affected by ATM inhibition, and chromosome-bound TPT1 was not detectable. Zhang et al. (2012) observed that downregulation of ATM in unirradiated AG1522 cells resulted in increased levels of TPT1 and suggested differential effects of ATM on TPT1 in irradiated and non-irradiated samples

[9]. According to that study, TPT1 forms complexes with ATM, γH2A.X and 53BP1 in chromatin-enriched fractions of osteosarcoma U2OS cells [9], but none of these proteins were pulled down in a more recent proteomic approach in HeLa cells [10]. In ADP fibroblasts and MCF10A breast epithelial cells, we did neither detect a significant enrichment of TPT1 in nuclear or chromatin fractions by western blot after IR, nor a prominent translocation of TPT1 to the nucleus by immunofluorescence analyses. Knockdown of TPT1 did not result in statistically significant changes of γH2A.X and 53BP1 foci numbers after IR. In agreement with these observations we did not detect a high fraction of TPT1 colocalizing with γH2A.X and no evidence for colocalization of TPT1 with RAD51 foci in wild-type human TERT-immortalized skin fibroblasts (BJ5TA), although a clear association between RAD51 and TPT1 has been recently shown using a proteomics approach in HeLa cells [30]. Forcomparison, colocalization between γH2A.X and 53BP1 can be up to 100% [44,45]. Although a spotty pattern of TPT1 was observed in both cell lines with both TPT1 antibodies, this pattern was different from foci, did not increase after IR and could similarly be detected in the cytoplasm of the cells. Our findings that TPT1 was not enriched in chromatin fractions after IR in several cell lines is consistent with the absence of radiation-induced TPT1 foci. TPT1 has previously been reported to show a granular localization pattern in the vicinity of and around the nucleus in ovarian epithelial cells and a spotty pattern in ovarian carcinoma cells while being present in the cell nucleus or cell periphery in other cell types [46], and there is further evidence for cell type dependent variation [4,9,47]. In this work, we provide evidence for a localization of TPT1 to the vicinity of the nucleus rather than its reported nuclear translocation after irradiation in several cellular systems. The role of TPT1 in apoptosis and cancer development has been recurrently described in the literature, however its precise involvement in both processes may be complex, as a p53-dependent induction of TPT1 can reduce oxidative stress, apoptosis and promote cell survival after hydrogen peroxide treatment [48], whereas elevated levels of TPT1 have been correlated with cancer development (reviewed in [3]). For example, its expression can be increased dramatically during oxidative stress [36], while our study does not confirm an induction after irradiation. Taken together, these data suggest that the effects of TPT1 are diverse and may depend on cell type and cellular status. Although our results on ADP fibroblasts and MCF10A breast epithelial cells were largely similar, we noticed a subtle delay in foci disappearance after TPT1 silencing that was more pronounced in ADP compared to MCF10A cells. It is possible that the p53 inhibitory state of large T-transformed ADP fibroblasts has contributed to this cell type difference. In this study, we have mainly focused on the question whether TPT1 might influence ATM signaling – a very important, yet not the only player in the DNA damage response. TPT1 could also exert an effect on DNA repair in the context of the ATR Serine/Threonine Kinase or DNA-PK signaling, as TPT1 has been shown to bind to the DNA-binding subunits, Ku70 and Ku80, of the DNA-PK [9]. Further work is needed to analyze a possible role of TPT1 in the DNA damage response independent of ATM signaling and reveal the reasons for cell type dependent variation of TPT1 function.

4.1. Conclusions

In summary, we have presented various lines of evidence from which we conclude that TPT1, an important biomarker in different cancers, may have subtle effects on overall breast cancer risk, as the potentially damaging mutation c.452A > G (p.Y151C) seems to be of rare occurrence, and its role in the course of DNA double strand break repair through ATM signaling is limited. Our results suggest that alterations in TPT1 levels do not grossly affect DNA

repair capacity after ionizing radiation in the analyzed cell systems but further work needs to be performed to reveal the reasons for discrepancies between published studies and cell type dependent variation.

Acknowledgement

Conflict of interest

We declare no conflict of interest.

Appendix A. Supplementary data

Supplementary data to this article can be found online at https://doi.org/10.1016/j.ctro.2019.01.006.

References

[1] Li F, Zhang D, Fujise K. Characterization of fortilin, a novel antiapoptotic protein. J Biol Chem 2001;276.

[2] Bommer U. The translational controlled tumour protein TCTP: biological functions and regulation. Results Probl Cell Differ 2017;64:69–126.

[3] Koziol MJ, Gurdon JB. TCTP in development and cancer. Biochem Res Int 2012;2012:105203. PubMed PMID: 22649730. PMCID: 3357502. Epub 2012/06/01. eng.

[4] Tuynder M, Susini L, Prieur S, Besse S, Fiucci G, Amson R, et al. Biological models and genes of tumor reversion: cellular reprogramming through tpt1/TCTP and SIAH-1. PNAS 2002:99.

[5] Telerman A, Amson R. The molecular programme of tumour reversion: the steps beyond malignant transformation. Nat Rev Cancer 2009;9.

[6] Bae SY, Kim HJ, Lee KJ, Lee K. Translationally controlled tumor protein induces epithelial to mesenchymal transition and promotes cell migration, invasion and metastasis. Sci Rep 2015;5:8061. PubMed PMID: 25622969. PMCID: 4306963. Epub 2015/01/28. eng.

[7] Acunzo J, Baylot V, So A, Rocchi P. TCTP as therapeutic target in cancers. Cancer Treat Rev. 2014;40(6):760–9. PubMed PMID: 24650927. Epub 2014/03/22. eng.

[8] Rho SB, Lee JH, Park MS, Byun H-J, Kang S, Seo S-S, et al. Anti-apoptotic protein TCTP controls the stability of the tumor suppressor p53. FEBS Lett 2011;585 (1):29–35.

[9] Zhang J, de Toledo SM, Pandey BN, Guo G, Pain D, Li H, et al. Role of the translationally controlled tumor protein in DNA damage sensing and repair. Proc Natl Acad Sci USA 2012;109(16):26.

[10] Li S, Chen M, Xiong Q, Zhang J, Cui Z, Ge F. Characterization of the Translationally Controlled Tumor Protein (TCTP) Interactome Reveals Novel Binding Partners in Human Cancer Cells. J Proteome Res 2016;15 (10):3741–51.

[11] Li SJ, Jia HY, Wu D, Fan ZM. Expression of translationally controlled tumor protein in human breast cancer and its clinical significance. Nan Fang Yi Ke Da Xue Xue Bao 2011;31(9):1560–3. PubMed PMID: 21945766. Epub 2011/09/29. chi.

[12] Amson R, Pece S, Lespagnol A, Vyas R, Mazzarol G, Tosoni D, et al. Reciprocal repression between P53 and TCTP. Nat Med 2011;18(1):91–9.

[13] Funston G, Goh W, Wei SJ, Tng QS, Brown C, Jiah Tong L, et al. Binding of Translationally Controlled Tumour Protein to the N-terminal domain of HDM2 is inhibited by nutlin-3. PLoS One 2012;7(8):e42642. PubMed PMID: 22912717. PMCID: 3418249. Epub 2012/08/23. eng.

[14] Reuter T, Medhurst A, Waisfisz Q, Zhi Y, Herterich S, Hoehn H, et al. Yeast two-hybrid screens imply involvement of fanconi anemia proteins in transcription regulation, cell signaling, oxidative metabolism, and cellular transport. Exp Cell Res 2003;289(2):211–21.

[15] Pukkala E, Kesminiene A, Poliakov S, Ryzhov A, Drozdovitch V, Kovgan L, et al. Breast cancer in Belarus and Ukraine after the Chernobyl accident. Int J Cancer 2006;119(3):651–8. PubMed PMID: 16506213. Epub 2006/03/01. eng.

[16] Wu D, Guo Z, Min W, Zhou B, Li M, Li W, et al. Upregulation of TCTP expression in human skin squamous cell carcinoma increases tumor cell viability through anti-apoptotic action of the protein. Exp Ther Med 2012;3:437–42.

[17] Lucibello M, Gambacurta A, Zonfrillo M, Pierimarchi P, Serafino A, Rasi G, et al. TCTP is a critical survival factor that protects cancer cells from oxidative stress-induced cell-death. Exp Cell Res 2011;317(17):2479–89. PubMed PMID: 21801721. Epub 2011/08/02. eng.

[18] Bogdanova N, Sokolenko AP, Iyevleva AG, Abysheva SN, Blaut M, Bremer M, et al. PALB2 mutations in German and Russian patients with bilateral breast cancer. Breast Cancer Res Treat 2011;126(2):545–50. PubMed PMID: 21165770. PMCID: 3291835. Epub 2010/12/18. eng.

[19] Ng P, Henikoff S. Predicting deleterious amino acid substitutions. Genome Res 2001;11(5):863–74.

[20] Choi Y, Sims G, Murphy S, Miller J, Chan A. Predicting the functional effect of amino acid substitutions and indels. PLoS One 2012;7(10):e46688. Epub 2012 Oct 8.

[21] Schwarz J, Cooper D, Schuelke M, Seelow D. MutationTaster2: mutation prediction for the deep-sequencing age. Nat Methods 2014;11(4):361–2.

[22] Adzhubei IA, Schmidt S, Peshkin L, Ramensky WE, Gerasimova A, Bork P, et al. A method and server for predicting damaging missense mutations. Nat Methods 2010;7.

[23] Schuelke M, Schwarz J, Seelow D. MutationTaster statistics – cross comparison. 2014 Accessed 12/18, 2018.

[24] Soule HD, Maloney TM, Wolman SR, Peterson Jr WD, Brenz R, McGrath CM, et al. Isolation and characterization of a spontaneously immortalized human breast epithelial cell line, MCF-10. Cancer Res 1990;50(18):6075–86. PubMed PMID: 1975513. Epub 1990/09/25. eng.

[25] Li X, Lee YK, Jeng JC, Yen Y, Schultz DC, Shih HM, et al. Role for KAP1 serine 824 phosphorylation and sumoylation/desumoylation switch in regulating KAP1-mediated transcriptional repression. J Biol Chem 2007;282(50):36177–89. PubMed PMID: 17942393. Epub 2007/10/19. eng.

[26] White D, Rafalska-Metcalf IU, Ivanov AV, Corsinotti A, Peng H, Lee SC, et al. The ATM substrate KAP1 controls DNA repair in heterochromatin: regulation by HP1 proteins and serine 473/824 phosphorylation. Mol Cancer Res: MCR 2012;10(3):401–14. PubMed PMID: 22205726. PMCID: 4894472. Epub 2011/12/30. eng.

[27] White DE, Negorev D, Peng H, Ivanov AV, Maul GG, Rauscher 3rd FJ. KAP1, a novel substrate for PIKK family members, colocalizes with numerous damage response factors at DNA lesions. Cancer Res 2006;66(24):11594–9. PubMed PMID: 17178852. Epub 2006/12/21. eng.

[28] Ziv Y, Bielopolski D, Galanty Y, Lukas C, Taya Y, Schultz DC, et al. Chromatin relaxation in response to DNA double-strand breaks is modulated by a novel ATM- and KAP-1 dependent pathway. Nat Cell Biol 2006;8(8):870–6. PubMed PMID: 16862143. Epub 2006/07/25. eng.

[29] Buscemi G, Carlessi L, Zannini L, Lisanti S, Fontanella E, Canevari S, et al. DNA damage-induced cell cycle regulation and function of novel Chk2 phosphoresidues. Mol Cell Biol 2006;26(21):7832–45. PubMed PMID: 16940182. PMCID: 1636737. Epub 2006/08/31. eng.

[30] Li Y, Sun H, Zhang C, Liu J, Zhang H, Fan F, et al. Identification of translationally controlled tumor protein in promotion of DNA homologous recombination repair in cancer cells by affinity proteomics. Oncogene 2017. PubMed PMID: 28846114. Epub 2017/08/29. eng.

[31] Deng SS, Xing TY, Zhou HY, Xiong RH, Lu YG, Wen B, et al. Comparative proteome analysis of breast cancer and adjacent normal breast tissues in human. Genomics Proteomics Bioinformatics 2006;4(3):165–72. PubMed PMID: 17127214. Epub 2006/11/28. eng.

[32] Chen C, Deng Y, Hua M, Xi Q, Liu R, Yang S, et al. Expression and clinical role of TCTP in epithelial ovarian cancer. J Mol Histol 2015;46(2):145–56. PubMed PMID: 25564355. Epub 2015/01/08. eng.

[33] Yachdav G, Kloppmann E, Kajan L, Hecht M, Goldberg T, Hamp T, et al. PredictProtein–an open resource for online prediction of protein structural and functional features. Nucleic Acids Res 2014;42 (Web Server issue):W337-43.

[34] Lee JH, Goodarzi AA, Jeggo PA, Paull TT. 53BP1 promotes ATM activity through direct interactions with the MRN complex. EMBO J 2010;29(3):574–85. PubMed PMID: 20010693. PMCID: 2830698. Epub 2009/12/17. eng.

[35] Burma S, Chen BP, Murphy M, Kurimasa A, Chen DJ. ATM phosphorylates histone H2AX in response to DNA double-strand breaks. J Biol Chem 2001;276 (45):42462–7. PubMed PMID: 11571274. Epub 2001/09/26. eng.

[36] Gnanasekar M, Ramaswamy K. Translationally controlled tumor protein of Brugia malayi functions as an antioxidant protein. Parasitol Res 2007;101 (6):1533–40. PubMed PMID: 17687568. PMCID: 2366903. Epub 2007/08/10. eng.

[37] Susini L, Besse S, Duflaut D, Lespagnol A, Beekman C, Fiucci G, et al. TCTP protects from apoptotic cell death by antagonizing bax function. Cell Death Differ 2008;15.

[38] Hong ST, Choi KW. TCTP directly regulates ATM activity to control genome stability and organ development in Drosophila melanogaster. Nat Commun 2013;4:2986. PubMed PMID: 24352200. Epub 2013/12/20. eng.

[39] Lossaint G, Besnard E, Fisher D, Piette J, Dulić V. Chk1 is dispensable for G2 arrest in response to sustained DNA damage when the ATM/p53/p21 pathway is functional. Oncogene 2011;30(41):4261–74.

[40] Zhang X, Li J, Sejas D, Pang Q. The ATM/p53/p21 Pathway Influences Cell Fate Decision between Apoptosis and Senescence in Reoxygenated Hematopoietic Progenitor Cells. J Biol Chem 2005;280(20):19635–40.

[41] el-Deiry W, Tokino T, Velculescu V, Levy D, Parsons R, Trent J, et al. WAF1, a potential mediator of p53 tumor suppression. Cell 1993;75(4):817–25.

[42] Aliouat-Denis C, Dendouga N, Van den Wyngaert I, Goehlmann H, Steller U, van de Weyer I, et al. p53-independent regulation of p21Waf1/Cip1 expression and senescence by Chk2. Mol Cancer Res 2005;3(11):627–34.

[43] Abbas T, Dutta A. p21 in cancer: intricate networks and multiple activities. Nat Rev Cancer 2009;9(6):400–14.

[44] Rappold I, Iwabuchi K, Date T, Chen J. Tumor suppressor p53 binding protein 1 (53BP1) is involved in DNA damage-signaling pathways. J Cell Biol. 2001;153 (3):613–20. PubMed PMID: 11331310. PMCID: 2190566. Epub 2001/05/02. eng.

[45] Schultz LB, Chehab NH, Malikzay A, Halazonetis TD. p53 binding protein 1 (53BP1) is an early participant in the cellular response to DNA double-strand breaks. J Cell Biol 2000;151(7):1381–90. PubMed PMID: 11134068. PMCID: 2150674. Epub 2001/01/03. eng.

[46] Kloc M, Tejpal N, Sidhu J, Ganachari M, Flores-Villanueva P, Jennings NB, et al. Inverse relationship between TCTP/RhoA and p53/cyclin A/actin expression in ovarian cancer cells. Folia Histochem Cytobiol 2012;50(3):358–67. PubMed PMID: 23042265. PMCID: 3753092. Epub 2012/10/09. eng.

[47] Baylot V, Katsogiannou M, Andrieu C, Taieb D, Acunzo J, Giusiano S, et al. Targeting TCTP as a new therapeutic strategy in castration-resistant prostate cancer. Mol Ther 2012;20(12):2244–56. PubMed PMID: 22893039. PMCID: 3519986. Epub 2012/08/16. eng.

[48] Chen W, Wang H, Tao S, Zheng Y, Wu W, Lian F, et al. Tumor protein translationally controlled 1 is a p53 target gene that promotes cell survival. Cell Cycle 2013;12(14):2321–8. PubMed PMID: 24067374. PMCID: 3755082. Epub 2013/09/27. eng.

[49] Küper L. Varianten des TCTP-Gens bei weißrussischen Patientinnen mit Mammakarzinom. Hannover: Hannover Medical School; 2017.

[50] Neuhäuser K. Impact of the DNA damage response in clinical and cellular radiosensitivity of cancer patients. Hannover: Hannover Medical School; 2018.